Quaternary Geochronology 34 (2016) 1–11

Contents lists available at ScienceDirect

Quaternary Geochronology

journal homepage: www.elsevier.com/locate/quageo

Research paper

Boulder height – exposure age relationships from a global glacial ^{10}Be compilation

Jakob Heyman [a, *], Patrick J. Applegate [b], Robin Blomdin [c], Natacha Gribenski [c], Jonathan M. Harbor [c, d], Arjen P. Stroeven [c]

[a] Department of Earth Sciences, University of Gothenburg, Sweden
[b] Earth and Environmental Sciences Institute, Pennsylvania State University, USA
[c] Geomorphology and Glaciology, Department of Physical Geography and Bolin Centre for Climate Research, Stockholm University, Sweden
[d] Department of Earth, Atmospheric, and Planetary Sciences, Purdue University, USA

ARTICLE INFO

Article history:
Received 16 October 2015
Received in revised form
8 March 2016
Accepted 10 March 2016
Available online 14 March 2016

Keywords:
Cosmogenic dating
Glacial boulder
Boulder height
Exposure age clustering

ABSTRACT

Cosmogenic exposure dating of glacial boulders is commonly used to estimate the timing of past glaciations because the method enables direct dating of the duration a boulder has been exposed to cosmic rays. For successful dating, the boulders must have been fully shielded from cosmic rays prior to deposition and continuously exposed to cosmic rays ever since. A common assumption is that boulder height (the distance between the top of the boulder and the surrounding surface) is important, and that tall boulders are more likely to have been continuously exposed to cosmic rays than short boulders and therefore yield more accurate exposure ages. Here we test this assumption based on exposure age clustering for groups of glacial boulders (and single cobbles) ^{10}Be exposure ages that have recorded boulder heights (3741 boulders; 579 boulder groups with ≥3 boulders). Of the full set of boulder groups with ≥3 boulders, 21% fulfill a reduced chi square criterion ($\chi^2_R < 2$) for well-clustered exposure ages. For boulder groups containing only tall boulders, the fraction of well-clustered exposure age groups is consistently larger. Moreover, this fraction of well-clustered exposure age groups increases with the minimum boulder height in each group. This result confirms the common assumption that tall boulders are generally better targets for cosmogenic exposure dating compared to short boulders. Whereas the tall boulder groups have a significantly larger fraction of well-clustered exposure age groups, there is nonetheless a dominant fraction (>50%) of the boulder groups with scattered exposure ages, highlighting the problem with prior and incomplete exposure for cosmogenic dating of glacial boulders.

1. Introduction

Cosmogenic exposure dating has become a key tool for glacial chronology studies, and exposure ages from formerly glaciated environments have been reported from all continents. Under ideal conditions, cosmogenic exposure dating can accurately and precisely yield the timing of glacial deposition or deglaciation, which can yield important data for paleoclimate reconstructions. More specifically, the samples must have been fully shielded from cosmic rays prior to glaciation (no prior exposure) and continuously exposed to the cosmic ray flux ever since deglaciation (no incomplete exposure). A major problem with cosmogenic exposure dating of glacial deposits is that samples often have experienced some prior and/or incomplete exposure, resulting in too-old or too-young exposure ages, respectively (Heyman et al., 2011b). Several processes and conditions can lead to prior exposure and incomplete exposure. Prior exposure can be the result of limited glacial erosion, leaving previously exposed surfaces intact, or the glacier picking up and depositing material that was previously exposed to cosmic rays at the ground surface or at shallow depths. Incomplete exposure can be the result of multiple processes leading to a shielding history of the present-day surface under sediments, snow, water, or bedrock. A common strategy to evaluate whether prior and/or incomplete exposure has affected the samples is to date multiple samples from each single site. Scattered exposure ages in single-site sample groups are typically interpreted to reflect prior and/or incomplete exposure; well-clustered exposure ages are typically interpreted as yielding the actual deglaciation age (Balco, 2011).

* Corresponding author.
E-mail address: jakob.heyman@gu.se (J. Heyman).

http://dx.doi.org/10.1016/j.quageo.2016.03.002
1871-1014/

Perhaps the most common strategy for cosmogenic dating of glacial landforms is to date samples from the top of glacially transported boulders located on moraines or in the open landscape. Glacially transported boulders are ubiquitous in formerly glaciated regions and their importance for understanding glacier expansion has been recognized since the early days of paleoglaciology (Fig. 1; Charpentier, 1841). Because glacial boulders have potentially been plucked, crushed, and abraded, the risk of prior exposure is often lower than for bedrock samples. This has been shown for regions of the Fennoscandian and Laurentide ice sheets preserved under non-erosive ice with significantly less prior exposure in boulders compared to bedrock surfaces (Fabel et al., 2002; Briner et al., 2006; Goehring et al., 2008). Regarding incomplete exposure, two main processes for glacial boulders are landscape degradation, leading to exhumation of boulders through sediments, and toppling, bringing previously shielded boulder surfaces to the top (Hallet and Putkonen, 1994; Putkonen and Swanson, 2003; Applegate et al., 2010, 2012; Heyman et al., 2011b). For both of these processes (and also for snow coverage), sampling of large boulders that protrude well above the surrounding surface should theoretically reduce the risk of incomplete exposure as a large and tall boulder is more likely to have evaded coverage by sediment and has likely been more stable than a small boulder. Hence, a common strategy for cosmogenic dating of glacial boulders is to choose the largest and tallest boulders for sample collection and boulder size/height is often used as a sampling criterion (e.g. Gosse et al., 1995; Kaplan et al., 2004; Kerschner et al., 2006; Applegate and Alley, 2011; Houmark-Nielsen et al., 2012; Lifton et al., 2014a; Nývlt et al., 2014; Bromley et al., 2015; Corbett et al., 2015; Doughty et al., 2015).

The influence of boulder size on exposure age has been investigated in some local studies (Blard et al., 2007; Briner, 2009), but this has not been attempted for larger datasets. To fill this gap, we present a comprehensive compilation of ^{10}Be exposure ages from glacial boulders that also include data on boulder height (the distance between the top of the boulder and the surrounding surface). The objective is to test the common assumption that tall boulders yield more accurate exposure ages, and to evaluate the potential effect of boulder height on exposure age.

2. Methods

2.1. Data compilation

We have compiled boulder height and ^{10}Be exposure age data for glacial boulders (Table 1) with some additional data derived from communication with the original authors. Included are all glacial boulders and single clast cobbles with ^{10}Be and boulder/cobble height data (Fig. 2). We include single clast cobbles under the boulder umbrella because the size criterion for differentiating cobbles from boulders is applied somewhat arbitrarily and in many publications remain not well-defined. Obvious data errors, including mistaken coordinates and ^{10}Be concentrations with incorrect exponents, have been corrected. For samples with no reported density, we assume a density of 2.65 g cm^{-3}. For samples located in mountain regions and lacking topographic shielding data, we have calculated topographic shielding factors from 30 to 90 m resolution elevation models based on Codilean (2006) and Li (2013). Year of sampling (used in the exposure age calculation to adjust the time-dependent spallation production rate) is based on sample names and information in the source publication if available, and is otherwise assumed to be two years before publication. All sample data is available in the Supplementary Dataset.

To calculate zero erosion exposure ages, we use a modified version of the CRONUS calculator (Balco et al., 2008) code, with ^{10}Be production based on the nuclide-specific LSD spallation and muon production rate scaling (Lifton et al., 2014b) and the muon production parameterization of Phillips et al. (2016a). We use a reference ^{10}Be spallation production rate of 3.98 ± 0.17 atoms g^{-1} yr^{-1}, based on a global compilation of 22 well-clustered ^{10}Be production rates (Supplementary Fig. S1; Supplementary Dataset). This reference production rate matches well with the nuclide-specific LSD scaling reference production rates of Shakun et al. (2015) (4.0 ± 0.1 atoms g^{-1} yr^{-1}) and Phillips et al. (2016a) (3.92 ± 0.31 atoms g^{-1} yr^{-1}), based on subsets of the data used here for production rate calibration. Using a global average reference production rate instead of locally calibrated reference production rates (cf. Balco et al., 2009) can yield some differences in the actual exposure ages but it will not affect the exposure age clustering of single site samples. More detailed information on the exposure age calculation and the production rate calibration is presented in the Supplementary Information. Because we are primarily interested in comparing exposure ages of multiple boulders from single sites with minor production rate variation we calculate and use internal exposure age uncertainties not including the production rate uncertainty (Balco et al., 2008). The code (Octave/Matlab) used for exposure age calculation is provided as supplementary material.

All ^{10}Be measurements (n = 3831) have been organized in 3741 numbered samples (including 134 cobbles) with repeat

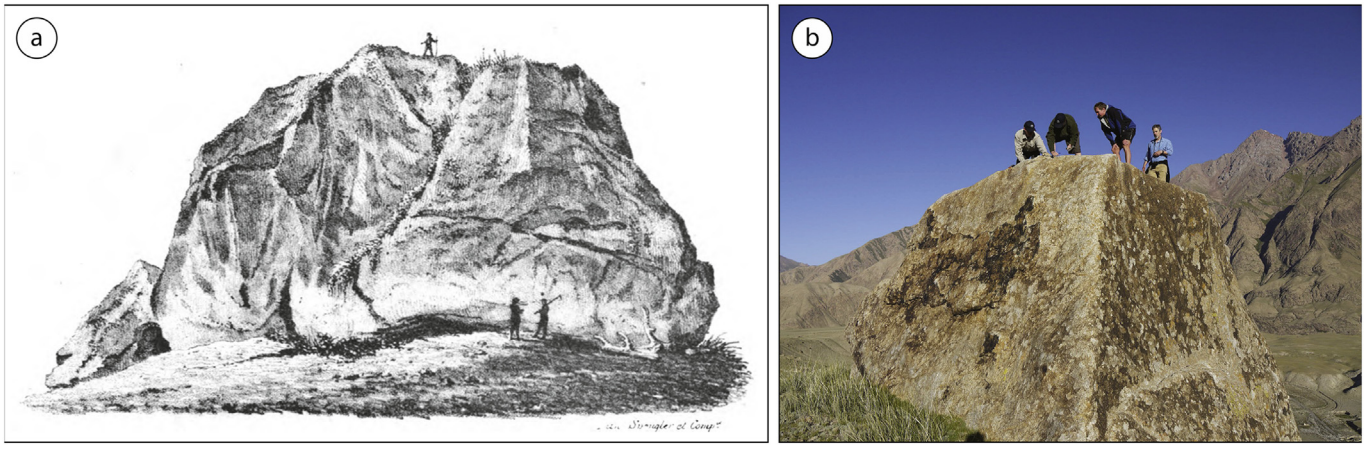

Fig. 1. (a) A large boulder in Pierre des Marmettes, Rhône Valley, Switzerland, recognized as a glacial erratic boulder by Charpentier (1841). This image is in the public domain. (b) Sampling of a tall boulder (boulder height of 4 m) for cosmogenic dating of a moraine in Tian Shan (Lifton et al., 2014a: sample INK-01B).

Table 1
Publications included in the data compilation, and the number of boulders with ^{10}Be and boulder height information. See Supplementary Dataset for sample ^{10}Be and boulder height data.

Publication	Boulders	Publication	Boulders	Publication	Boulders
Abbühl et al. (2009)	1	Henriksen et al. (2014)	9	Putnam et al. (2010b)	10
Abramowski (2004)	10	Heyman et al. (2011a)	39	Putnam et al. (2012)	45
Abramowski et al. (2006)	50	Hippe et al. (2014)	1	Putnam et al. (2013a)	39
Akçar et al. (2007)	17	Hormes et al. (2011)	11	Putnam et al. (2013b)	73
Akçar et al. (2008)	10	Hormes et al. (2013)	1	Rades et al. (2015)	11
Akçar et al. (2011)	3	Houmark-Nielsen et al. (2012)	30	Reber et al. (2014a)	7
Akçar et al. (2014)	41	Hughes et al. (2014)	8	Reber et al. (2014b)	40
Akçar et al. (in press)	28	Hughes et al. (2016)	1	Refsnider et al. (2008)	12
Alexanderson and Fabel (2015)	6	Ivy-Ochs et al. (1999)	5	Reuther (2007)	8
Badding et al. (2013)	9	Ivy-Ochs et al. (2004)	4	Reuther et al. (2007)	18
Balco et al. (2009)	18	Ivy-Ochs et al. (2006a)	7	Reuther et al. (2011)	16
Balco et al. (2013)	2	Ivy-Ochs et al. (2006b)	1	Rinterknecht et al. (2004)	9
Benson et al. (2004)	5	Ivy-Ochs et al. (2008)	11	Rinterknecht et al. (2005)	37
Benson et al. (2007)	25	Johnsen et al. (2009)	6	Rinterknecht et al. (2009)	10
Blard et al. (2013)	6	Jomelli et al. (2011)	59	Rother (2006)	7
Briner et al. (2003)	7	Jomelli et al. (2014)	39	Rother et al. (2014a)	56
Briner et al. (2005)	93	Joy et al. (2014)	18	Rother et al. (2014b)	20
Briner et al. (2007)	7	Kaplan et al. (2004)	13	Rother et al. (2015)	31
Bromley et al. (2015)	7	Kaplan et al. (2005)	22	Ruszkiczay-Rüdiger et al. (in press)	14
Brugger (2007)	7	Kaplan et al. (2007)	23	Sagredo et al. (2011)	4
Carcaillet et al. (2013)	11	Kaplan et al. (2008)	14	Saha et al. (in press)	10
Carlson et al. (2007)	13	Kelley et al. (2012)	1	Schaefer et al. (2006)	16
Chen et al. (2011)	5	Kelly et al. (2015)	2	Scherler et al. (2010)	24
Clark et al. (2009a)	8	Kerschner et al. (2006)	5	Schildgen (2000)	3
Clark et al. (2009b)	16	Kiernan et al. (2010)	12	Schindelwig et al. (2012)	23
Corbett et al. (2015)	28	Kiernan et al. (2014)	12	Seong et al. (2007)	65
Cronauer et al. (in press)	11	Laabs et al. (2007)	13	Seong et al. (2009)	124
Davis et al. (2006)	15	Laabs et al. (2009)	27	Shulmeister et al. (2005)	11
Di Nicola et al. (2009)	14	Laabs et al. (2011)	24	Shulmeister et al. (2010)	17
Dong et al. (2014)	15	Le Roy (2012)	27	Smith and Rodbell (2010)	57
Dortch et al. (2010a)	22	Lee et al. (2014)	24	Smith et al. (2005a)	132
Dortch et al. (2010b)	51	Li et al. (2014)	33	Smith et al. (2005b)	39
Doughty et al. (2015)	30	Licciardi and Pierce (2008)	68	Standell (2014)	6
Douglass et al. (2005)	14	Licciardi et al. (2009)	28	Storey et al. (2010)	25
Douglass et al. (2006)	38	Lifton et al. (2014a)	20	Strasky et al. (2006)	1
Engel et al. (2011)	7	Lindow et al. (2014)	5	Strasky et al. (2009)	5
Engel et al. (2014)	30	Mackintosh et al. (2007)	20	Stroeven et al. (2010)	33
Engel et al. (2015)	23	Mangerud et al. (2008)	11	Stroeven et al. (2014)	17
Fink et al. (2006)	11	Margold et al. (2014)	8	Svendsen et al. (2015)	14
Fogwill and Kubik (2005)	3	Margold et al. (2016)	18	Tschudi et al. (2000)	4
Fu et al. (2013)	49	Mathers (2014)	32	Tschudi et al. (2003)	2
García et al. (2012)	38	May et al. (2011)	16	Ullman et al. (2013)	2
Gheorghiu et al. (2015)	24	McCarthy et al. (2008)	2	Wang et al. (2013)	22
Gjermundsen et al. (2013)	11	McCulloch et al. (2005)	10	Ward et al. (2007)	5
Glasser et al. (2006)	3	Mentlík et al. (2013)	10	Wesnousky et al. (2012)	23
Glasser et al. (2009)	21	Moran et al. (in press)	9	White and Fink (2014)	7
Glasser et al. (2011)	10	Moreno et al. (2009)	11	White et al. (2011)	30
Glasser et al. (2014)	9	Munroe et al. (2006)	20	Wirsig et al. (2016)	4
Goehring et al. (2008)	29	Murari et al. (2014)	34	Yamane et al. (2011)	2
Golledge et al. (2007)	3	Murray et al. (2012)	21	Young et al. (2009)	23
Gosse et al. (1995)	14	Nývlt et al. (2014)	9	Young et al. (2011a)	4
Graf et al. (2007)	4	Owen et al. (2003)	18	Young et al. (2011b)	6
Graf et al. (2008)	17	Owen et al. (2005)	62	Young et al. (2012)	15
Graf et al. (2015)	17	Owen et al. (2006)	55	Young et al. (2013a)	2
Håkansson et al. (2007a)	4	Owen et al. (2009)	59	Young et al. (2013b)	12
Håkansson et al. (2007b)	5	Owen et al. (2010)	83	Zahno et al. (2009)	10
Håkansson et al. (2009)	36	Owen et al. (2012)	73	Zahno et al. (2010)	22
Hebenstreit et al. (2011)	6	Pendleton et al. (2015)	24	Zech et al. (2007)	8
Hedrick et al. (2011)	47	Phillips et al. (2008)	18	Zech et al. (2009)	35
Hein et al. (2009)	23	Phillips et al. (2016b)	10	Zech et al. (2010)	10
Hein et al. (2010)	9	Pratt-Sitaula et al. (2011)	24		
Hein et al. (2011)	13	Putnam et al. (2010a)	27		

measurements of samples from single boulders given the same sample number. For boulders with multiple ^{10}Be measurements we determine an error-weighted exposure age and uncertainty. All samples have been organized in numbered groups (n = 1180), with each group including boulders from one location with an expected single deglaciation age. Typical groups of samples consist of boulders collected from one moraine ridge, or boulders located in a confined region that is assumed to yield a single deglaciation age. The extent of these confined regions ranges from hundreds of meters for boulders deposited by small glaciers to 10–15 km for boulders deposited by retreating ice sheets. Fig. 3 presents the number of sample locations with a given boulder group size (number of boulders).

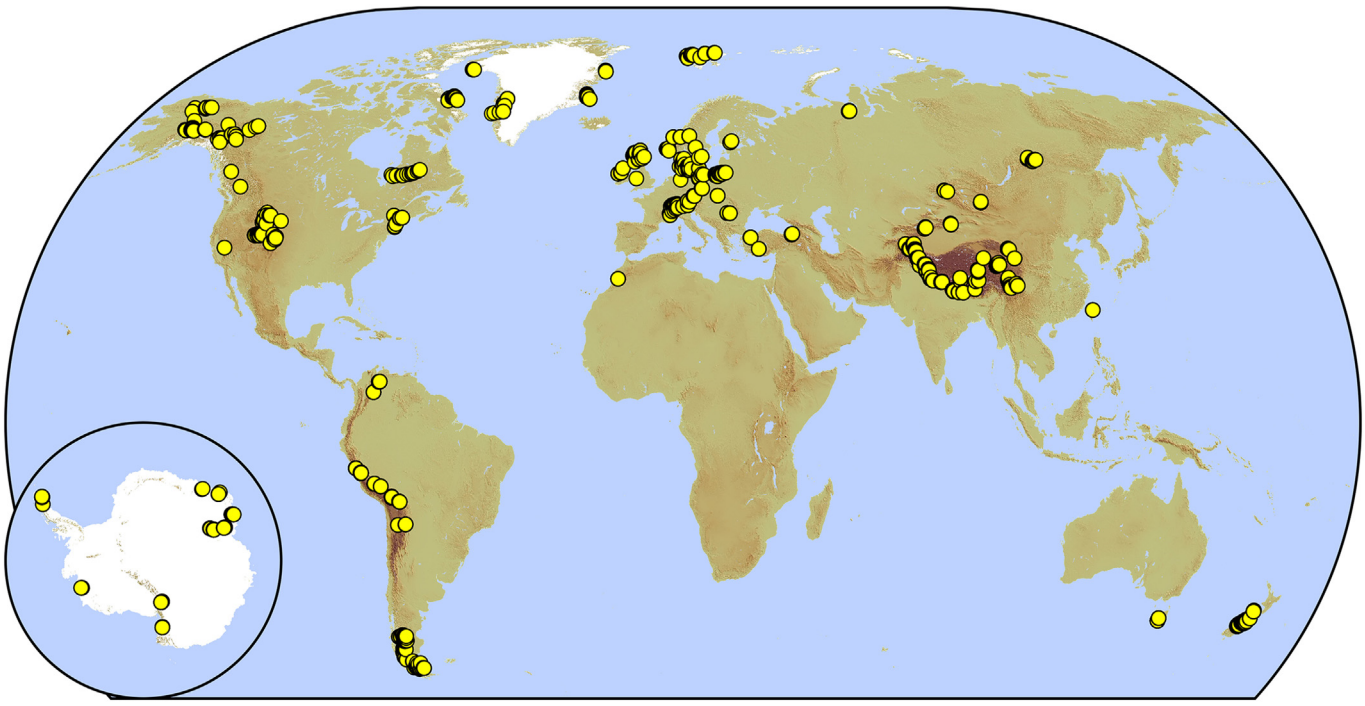

Fig. 2. Map showing the location of all boulders with recorded ^{10}Be exposure ages and boulder heights included in the compilation.

2.2. Data analysis

As a measure of boulder group exposure age quality, we use exposure age clustering, assuming that groups of well-clustered exposure ages contain high-quality exposure ages free from prior exposure and incomplete exposure errors. For all boulder groups with a minimum of three samples (n = 579; Fig. 3) we calculate the reduced chi square value (χ^2_R) as a measure of clustering:

$$\chi^2_R = \frac{1}{n-1}\sum_{i=1}^{n}\left(\frac{t_i - \bar{t}}{\sigma_i}\right)^2 \quad (1)$$

where n is the number of boulders in the boulder group, t_i is an individual boulder exposure age, $\bar{t}$ is the boulder group mean exposure age, and σ_i is the individual boulder exposure age uncertainty. The reduced chi square value increases with exposure age scatter and a value close to 1 is expected for a group of exposure ages with a scatter caused only by the measurement uncertainty (cf. Balco, 2011). We use a cut-off value of 2 to differentiate well-clustered ($\chi^2_R < 2$) from scattered ($\chi^2_R \geq 2$) exposure age groups. Using a constant reduced chi square cut-off value honors the group size (number of individual boulders per group), because the probability for a group of exposure ages with an age scatter causesed only by the measurement uncertainty increases with group size. Supplementary Fig. S2 illustrates the significance of group size and shows that the probability to fulfill ($\chi^2_R < 2$) for groups of three, five, and eight exposure ages drawn from one Gaussian distribution are 86%, 91%, and 95%, respectively. To investigate the influence of boulder height on exposure age quality, we first organize sub-sets of the boulder groups by boulder height, using boulder height cut-off values ranging from 20 cm to 300 cm and selecting all boulders above or at a boulder height cut-off value (tall groups) and all boulders below this boulder height cut-off value (short groups), still requiring a minimum of three boulders per group. We then quantify the fraction of boulder groups with $\chi^2_R < 2$ (well-clustered) for both the tall and the short groups for all boulder height cut-off values (adopting increments of 20 cm). To evaluate the effects on exposure age quality of prior exposure and incomplete exposure in relation to boulder height, we calculate the age ratio between the excluded short/tall boulders and the average group exposure age of the remaining tall/short boulders for all well-clustered ($\chi^2_R < 2$) tall/short exposure age groups that have scattered ($\chi^2_R \geq 2$) exposure ages before excluding the short/tall boulders (Supplementary Fig. S3).

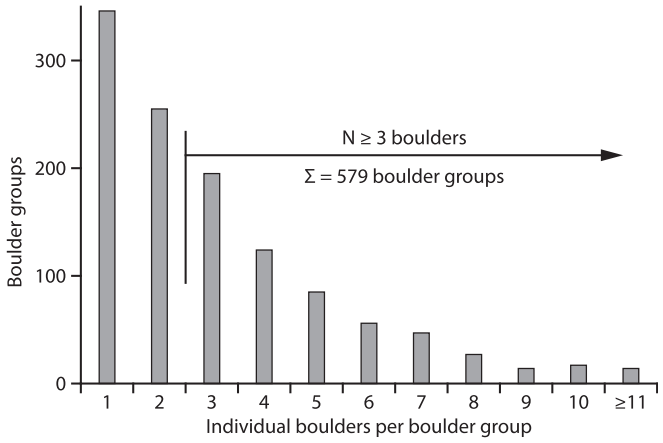

Fig. 3. Number of boulder groups against number of individual boulders per boulder group. There are 579 boulder groups with at least three individual boulders included in the analysis of exposure age clustering (Figs. 4–7).

If indeed tall boulders generally yield more accurate exposure ages, as suggested and implied in many papers, we expect that a larger fraction of the tall boulder groups should have well-clustered exposure ages. If this is true and the reason is that short boulders are more likely to have been shielded from cosmic rays since deposition, we expect that the short boulders excluded from the well-clustered tall boulder exposure age groups should be

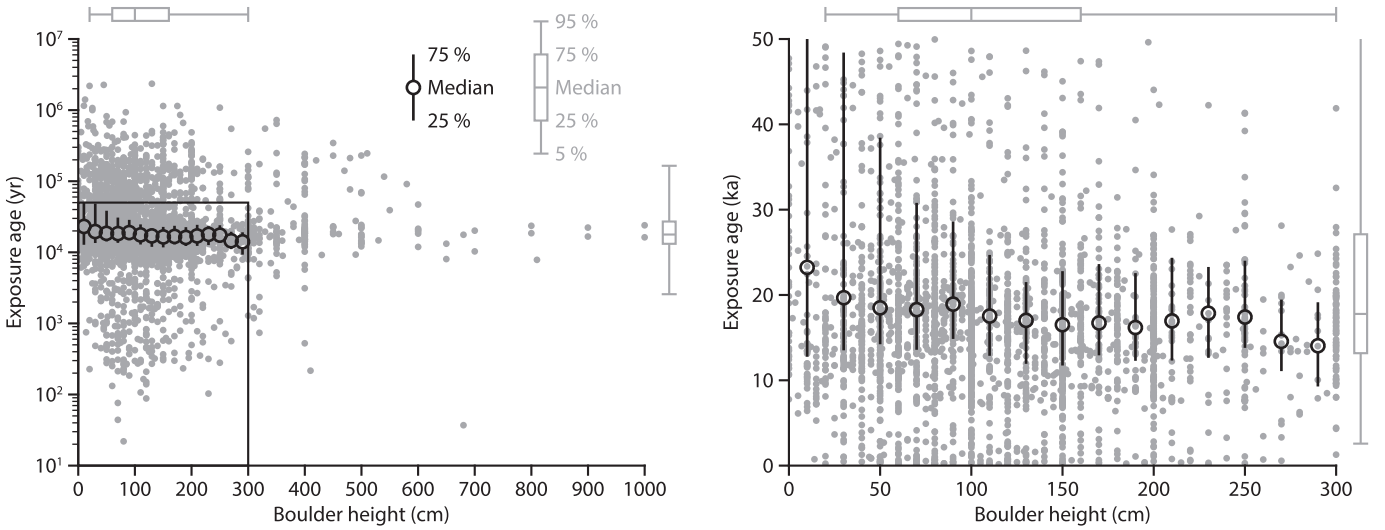

Fig. 4. Exposure age versus boulder height for the full set of individual glacial boulders in the compilation. The black symbols (circles and lines) show the median exposure age and interquartile range for the boulders with boulder heights in the range 0–300 cm divided into 15 intervals of 20 cm. The gray box and whisker plots summarize the exposure age and boulder height data for the full dataset. Note that the exposure age data is shown with a logarithmic scale in the left panel but with a linear scale in the right panel.

dominated by exposure ages younger than the associated tall boulder mean exposure ages.

3. Results

The dated boulders and cobbles have reported heights ranging from 0 to 1000 cm with a median of 100 cm and 50% of the boulders residing in the 60–160 cm interval. The exposure ages range from 22 to 2.3 × 10^6 years with a median of 18 ka and 50% of the exposure ages falling in the 13 to 27 ka interval (Fig. 4). For boulders taller than 100 cm, 50% of the exposure ages range from 13 ka to 24 ka, while for boulders shorter than 100 cm the fraction of older exposure ages increases with shorter boulders. Fig. 5 shows the boulder group χ^2_R values versus mean exposure age. The time range with the most and largest fraction of well-clustered boulder exposure age groups is 10–15 ka. Hence, boulder groups with both older and younger mean exposure ages show more scatter.

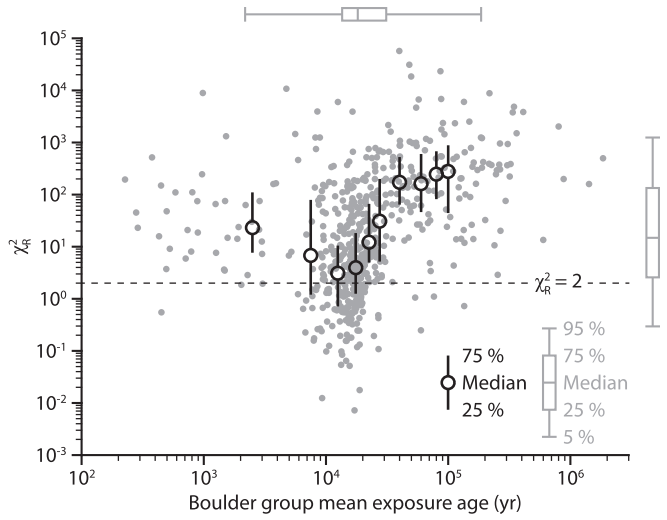

Fig. 5. Exposure age reduced chi square value (χ^2_R) versus mean exposure age for all boulder groups with at least three individual boulders shown in a log–log graph. The black symbols (circles and lines) show the median reduced chi square value and interquartile range for boulder group mean exposure ages with intervals of 5 ka for the range 0–30 ka, and with intervals of 20 ka for the range 30–110 ka. The gray box and whisker plots summarize the reduced chi square and mean exposure age data for the full dataset. The dashed horizontal line marks the reduced chi square value ($\chi^2_R = 2$) used to differentiate the well-clustered from the scattered exposure age groups.

For the full boulder group dataset (n = 579), across the range of boulder heights, only 21% of the boulder groups are well-clustered with $\chi^2_R < 2$ (Fig. 6). The tall boulder groups, with all boulders equal to or taller than a boulder height cut-off value, consistently have a larger ratio of well-clustered exposure ages than the short boulder groups. For the tall boulder groups, the ratio of well-clustered exposure age groups increases from 21% for boulders ≥20 cm to 34% for boulders ≥160 cm. For the short boulder groups, the ratio of well-clustered exposure age groups ranges from 16% to 20% for boulders <80–300 cm and becomes as low as 10% for boulders <60 cm.

Fig. 7 shows the summed probability density distribution of the exposure age ratio between the excluded short boulders and the well-clustered tall boulder group mean exposure ages (red curves) and the exposure age ratio between the excluded tall boulders and well-clustered short boulder group mean exposure ages (blue curves) for boulder height cut-off values of 80–140 cm. The excluded boulders are those for which exposure age groups change from scattered to well-clustered when excluded, and thus, this figure shows the tendency for outlier boulders to be affected by incomplete exposure (too young) or prior exposure (too old). For the excluded short boulders, there is an overweight for incomplete exposure (younger excluded boulder than well-clustered group mean exposure age) with 57–69% of the summed probability for boulder height cut-off values of 80–140 cm. For the excluded tall boulders, the exposure age ratio of the well-clustered short boulder group mean exposure age is more evenly distributed with 40–54% of the summed probability due to incomplete exposure for boulder height cut-off values of 80–140.

4. Discussion

Based on the boulder group exposure age clustering, the prediction that tall boulders should yield higher quality exposure ages is confirmed by the larger fraction of well-clustered exposure ages for the tall boulder groups (Fig. 6). The tall boulder groups have larger fractions of well-clustered exposure ages across all

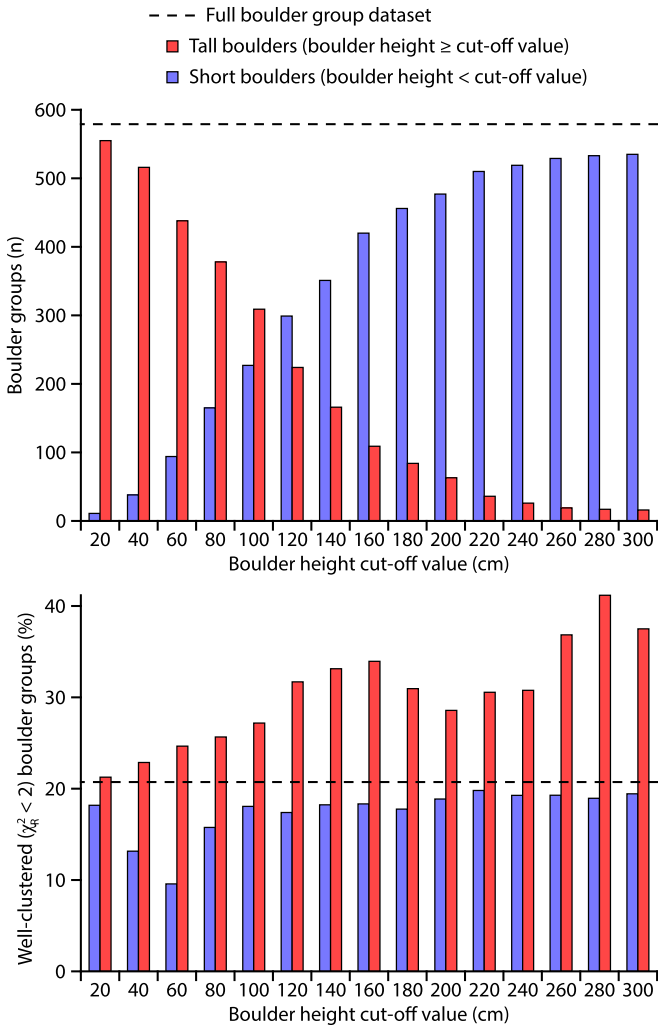

Fig. 6. Number of boulder groups (upper graph) with at least three individual boulders and fraction of well-clustered exposure age groups (lower graph) for tall (red) and short (blue) boulder groups defined by boulder height cut-off values ranging from 20 cm to 300 cm. The horizontal dashed lines show the full number of boulder groups (upper graph) and the fraction of well-clustered boulder groups of the full boulder group dataset (lower graph). See Section 2.2 for a complete explanation of the analysis. Supplementary Fig. S4 shows data for the same analysis but requiring a minimum group size of five individual boulders. Supplementary Fig. S5 shows data for the same analysis but only including boulder samples (excluding cobble samples). (For interpretation of the references to color in this figure legend, the reader is referred to the web version of this article.)

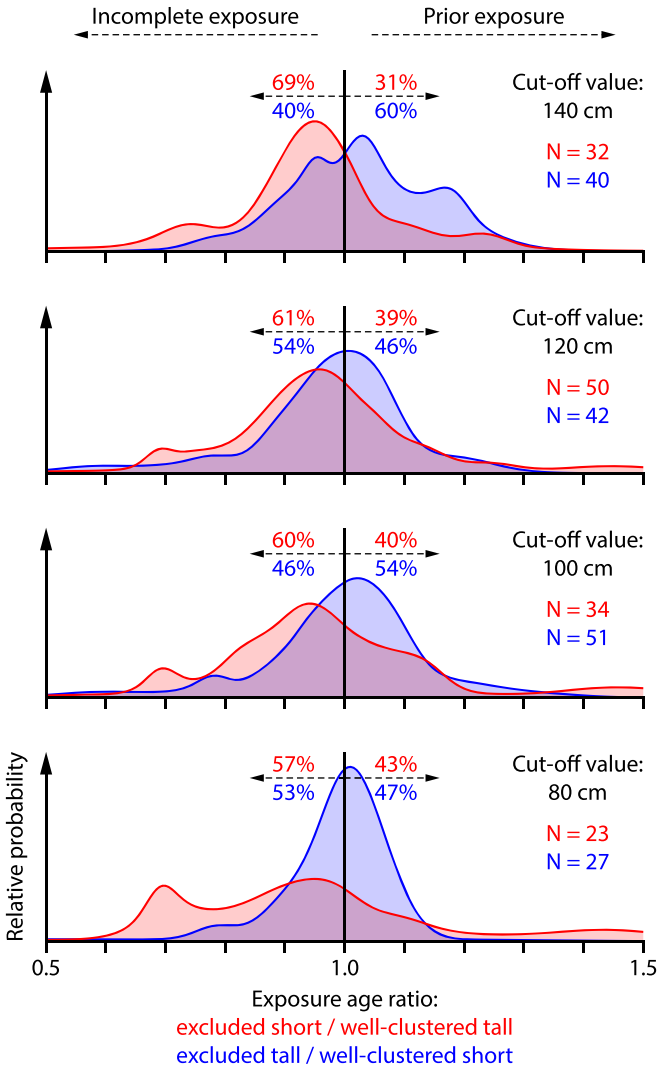

Fig. 7. Summed probability density curves for the exposure age ratio of excluded individual short/tall (red/blue) boulders divided by the well-clustered mean age of the remaining tall/short boulders for boulder height cut-off values of 80–140 cm. Only boulders that yield scattered exposure ages ($\chi^2_R \geq 2$) when included in boulder groups but for which, when excluded, the remaining boulders yield well-clustered exposure ages ($\chi^2_R < 2$) are included in the probability density curves. The red and blue values by the dashed arrows show ratios of the integrated summed probability below and above 1.0 for the excluded short and tall boulders. (For interpretation of the references to color in this figure legend, the reader is referred to the web version of this article.)

boulder height cut-off values than the short boulder groups or boulder groups including all boulder heights. Similarly, the short boulder groups have a consistently lower fraction of well-clustered exposure ages confirming a somewhat lower quality (more scatter) of derived exposure ages. For both the tall boulders and the short boulders, the fraction of well-clustered exposure age groups tends to increase with increasing boulder height cut-off values, supporting the prediction that taller boulders should yield higher quality exposure ages. In particular, the data shows a linear increase of the fraction of well-clustered tall boulder groups for boulder height cut-off values between 20 and 160 cm (Fig. 6).

For the short boulders which when included yield scattered boulder group exposure ages and when excluded result in well-clustered boulder group exposure ages, there is a tendency for exposure ages to be younger than the tall boulders from the same boulder group (Fig. 7). This indicates a tendency for incomplete exposure dominating over prior exposure for these short boulders, in line with the common assumption that short boulders have been more prone to shielding from cosmic rays since deposition. The young exposure ages of the excluded short boulders contrast with the general tendency of a larger fraction of old exposure ages amongst short boulders (Fig. 4). This further strengthens the interpretation that short boulders are more prone to incomplete exposure. For tall boulders which when included yield scattered boulder group exposure ages and when excluded result in well-clustered exposure ages, there is no clear tendency for incomplete exposure or prior exposure (Fig. 7). However, the 60% summed probability in the prior exposure domain for the excluded tall boulders ≥140 cm could possibly be interpreted as a result of supraglacial transportation of large boulders yielding prior exposure, as suggested by Darvill et al.

(2015).

The better clustering of the tall boulder group exposure ages is a clear and strong argument that, on average, tall boulders yield higher quality exposure ages. The increasing fraction of well-clustered exposure ages with increasing boulder height cut-off values shows that short boulders are more likely to have been shielded. In the present study we focus exclusively on boulder height and we therefore disregard other factors that could affect the exposure histories of the analyzed samples. It is possible that if more factors were taken into account (such as sample location or the nature of the substrate – is the boulder rooted in sediments or resting on bedrock?) the outcome could differ. However, the difference between the tall and the short boulders in terms of the fraction of well-clustered exposure age groups (Fig. 6) is clear enough to support the assertion that exposure ages from tall boulders are more likely to be correct than exposure ages from short boulders.

While tall boulders are clearly better clustered than short boulders, a large fraction of the tall boulder groups still yield scattered exposure ages, and thus collecting only tall boulders will not guarantee well-clustered exposure ages. Even for boulder heights equal to or in excess of 160 cm, only 36% of the boulder groups display well-clustered exposure ages (Fig. 6; Supplementary Dataset). Several processes and conditions can result in erroneous exposure ages through prior exposure or incomplete exposure, and excluding short boulders will only reduce some of the incomplete exposure problems. A major factor for the likelihood to obtain well-clustered exposure ages appears to be the age of the deposit (cf. Brown et al., 2005) as shown in Fig. 5. For boulder groups with mean exposure ages between 10 and 15 ka, 42% are well-clustered, while only 3% (4 out of 148) of the boulder groups with mean exposure ages older than 30 ka are well-clustered.

5. Conclusions

Based on a global compilation of glacial boulder ^{10}Be exposure ages and recorded boulder heights, we conclude that:

- Groups of tall boulders more often yield well-clustered high-quality exposure ages than groups of short boulders or groups including short boulders. The fraction of well-clustered exposure ages increases with boulder height cut-off values up to 160 cm. These data confirm the common assumption that tall boulders are more likely to have escaped post-glacial shielding and that tall boulders are therefore more likely to yield accurate exposure ages than short boulders.
- While groups of tall boulders often yield better clustered exposure ages, sampling only tall boulders does not resolve all issues with exposure age scatter due to prior and incomplete exposure. Even for groups of only tall boulders there is a large fraction of groups with scattered exposure ages. In particular, boulder groups with old exposure ages (>30 ka) are very rarely well-clustered.

Acknowledgments

We thank Vincent Rinterknecht and one anonymous reviewer for helpful reviews.

Appendix A. Supplementary data

Supplementary data related to this article can be found at http://dx.doi.org/10.1016/j.quageo.2016.03.002.

References

Abbühl, L.M., Akçar, N., Strasky, S., Graf, A.A., Ivy-Ochs, S., Schlüchter, C., 2009. A zero-exposure time test on an erratic boulder: evaluating the problem of pre-exposure in surface exposure dating. Eiszeitalt. Ggw. Quat. Sci. J. 58, 1–11.

Abramowski, U., 2004. The Use of ^{10}Be Surface Exposure Dating of Erratic Boulders in the Reconstruction of the Late Pleistocene Glaciation History of Mountainous Regions, with Examples from Nepal and Central Asia (PhD thesis). University of Bayreuth.

Abramowski, U., Bergau, A., Seebach, D., Zech, R., Glaser, B., Sosin, P., Kubik, P.W., Zech, W., 2006. Pleistocene glaciations of central Asia: results from ^{10}Be surface exposure ages of erratic boulders from the Pamir (Tajikistan), and the Alay-Turkestan range (Kyrgyzstan). Quat. Sci. Rev. 25, 1080–1096.

Akçar, N., Yavuz, V., Ivy-Ochs, S., Kubik, P.W., Vardar, M., Schlüchter, C., 2007. Paleoglacial records from Kavron Valley, NE Turkey: field and cosmogenic exposure dating evidence. Quat. Int. 164–165, 170–183.

Akçar, N., Yavuz, V., Ivy-Ochs, S., Kubik, P.W., Vardar, M., Schlüchter, C., 2008. A case for a downwasting mountain glacier during termination I, Verçenik valley, northeastern Turkey. J. Quat. Sci. 23, 273–285.

Akçar, N., Ivy-Ochs, S., Kubik, P.W., Schlüchter, C., 2011. Post-depositional impacts on 'Findlinge' (erratic boulders) and their implications for surface-exposure dating. Swiss J. Geosci. 104, 445–453.

Akçar, N., Yavuz, V., Ivy-Ochs, S., Reber, R., Kubik, P.W., Zahno, C., Schlüchter, C., 2014. Glacier response to the change in atmospheric circulation in the eastern Mediterranean during the last glacial maximum. Quat. Geochronol. 19, 27–41.

Akçar, N., Yavuz, V., Yeşilyurt, S., Ivy-Ochs, S., Reber, R., Bayrakdar, C., Kubik, P.W., Zahno, C., Schlunegger, F., Schlüchter, C., 2016. Synchronous Last Glacial Maximum across the Anatolian Peninsula, vol. 433. Geological Society, London, Special Publications. http://dx.doi.org/10.1144/SP433.7 (in press).

Alexanderson, H., Fabel, D., 2015. Holocene chronology of the Brattforsheden delta and inland dune field, SW Sweden. Geochronometria 42, 1–16.

Applegate, P.J., Alley, R.B., 2011. Challenges in the use of cosmogenic exposure dating of moraine boulders to trace the geographic extents of abrupt climate changes: the Younger Dryas example. In: Rashid, H., Polyak, L., Mosley-Thompson, E. (Eds.), Abrupt Climate Change: Mechanisms, Patterns, and Impacts, vol. 193. AGU Geophys. Monogr. Ser, pp. 111–122.

Applegate, P.J., Urban, N.M., Laabs, B.J.C., Keller, K., Alley, R.B., 2010. Modeling the statistical distributions of cosmogenic exposure dates from moraines. Geosci. Model Dev. 3, 293–307.

Applegate, P.J., Urban, N.M., Keller, K., Lowell, T.V., Laabs, B.J.C., Kelly, M.A., Alley, R.B., 2012. Improved moraine age interpretations through explicit matching of geomorphic process models to cosmogenic nuclide measurements from single landforms. Quat. Res. 77, 293–304.

Badding, M.E., Briner, J.P., Kaufman, D.S., 2013. ^{10}Be ages of late Pleistocene deglaciation and neoglaciation in the north-central Brooks Range, Arctic Alaska. J. Quat. Sci. 28, 95–102.

Balco, G., 2011. Contributions and unrealized potential contributions of cosmogenic-nuclide exposure dating to glacier chronology, 1990–2010. Quat. Sci. Rev. 30, 3–27.

Balco, G., Stone, J.O., Lifton, N.A., Dunai, T.J., 2008. A complete and easily accessible means of calculating surface exposure ages or erosion rates from ^{10}Be and ^{26}Al measurements. Quat. Geochronol. 3, 174–195.

Balco, G., Briner, J., Finkel, R.C., Rayburn, J.A., Ridge, J.C., Schaefer, J.M., 2009. Regional beryllium-10 production rate calibration for late-glacial northeastern North America. Quat. Geochronol. 4, 93–107.

Balco, G., Schaefer, J.M., Brachfeld, S., de Batist, M., Domack, E., Gordon, A., Haran, T., Henriet, J.-P., Huber, B., Ishman, S., Jeong, S., King, M., Lavoi, C., Leventer, A., McCormick, M., Mosley-Thompson, E., Pettit, E., Scambos, T., Smith, C., Thompson, L., Truffer, M., van Dover, C., Vernet, M., Wellner, J., Yu, K., Zagorodnov, V., 2013. Exposure-age record of Holocene ice sheet and ice shelf change in the northeast Antarctic Peninsula. Quat. Sci. Rev. 59, 101–111.

Benson, L., Madole, R., Phillips, W., Landis, G., Thomas, T., Kubik, P., 2004. The probable importance of snow and sediment shielding on cosmogenic ages of north-central Colorado Pinedale and pre-Pinedale moraines. Quat. Sci. Rev. 23, 193–206.

Benson, L., Madole, R., Kubik, P., McDonald, R., 2007. Surface-exposure ages of Front Range moraines that may have formed during the Younger Dryas, 8.2 cal ka, and little ice age events. Quat. Sci. Rev. 26, 1638–1649.

Blard, P.-H., Lavé, J., Pik, R., Wagnon, P., Bourlès, D., 2007. Persistence of full glacial conditions in the central Pacific until 15,000 years ago. Nature 449, 591–594.

Blard, P.-H., Braucher, R., Lavé, J., Bourlès, D., 2013. Cosmogenic ^{10}Be production rate calibrated against ^{3}He in the high tropical Andes (3800–4900 m, 20–22° S). Earth Planet. Sci. Lett. 382, 140–149.

Briner, J.P., 2009. Moraine pebbles and boulders yield indistinguishable ^{10}Be ages: a case study from Colorado, USA. Quat. Geochronol. 4, 299–305.

Briner, J.P., Miller, G.H., Davis, P.T., Bierman, P.R., Caffee, M., 2003. Last glacial maximum ice sheet dynamics in arctic Canada inferred from young erratics perched on ancient tors. Quat. Sci. Rev. 22, 437–444.

Briner, J.P., Miller, G.H., Davis, P.T., Finkel, R.C., 2005. Cosmogenic exposure dating in arctic glacial landscapes: implications for the glacial history of northeastern Baffin Island, arctic Canada. Can. J. Earth Sci. 42, 67–84.

Briner, J.P., Miller, G.H., Davis, P.T., Finkel, R.C., 2006. Cosmogenic radionuclides from fiord landscapes support differential erosion by overriding ice sheets. Geol. Soc. Am. Bull. 118, 406–420.

Briner, J.P., Overeem, I., Miller, G., Finkel, R., 2007. The deglaciation of Clyde Inlet, northeastern Baffin Island, arctic Canada. J. Quat. Sci. 22, 223–232.
Bromley, G.R.M., Hall, B.L., Thompson, W.B., Kaplan, M.R., Garcia, J.L., Schaefer, J.M., 2015. Late glacial fluctuations of the Laurentide ice sheet in the White Mountains of Maine and New Hampshire, U.S.A. Quat. Res. 83, 522–530.
Brown, E.T., Molnar, P., Bourlès, D.L., 2005. Comment on "Slip-rate measurements on the Karakorum Fault may imply secular variations in Fault motion". Science 309, 1326.
Brugger, K.A., 2007. Cosmogenic ^{10}Be and ^{36}Cl ages from late Pleistocene terminal moraine complexes in the Taylor River drainage basin, central Colorado, USA. Quat. Sci. Rev. 26, 494–499.
Carcaillet, J., Angel, I., Carrillo, E., Audemard, F.A., Beck, C., 2013. Timing of the last deglaciation in the Sierra Nevada of the Mérida Andes, Venezuela. Quat. Res. 80, 482–494.
Carlson, A.E., Clark, P.U., Raisbeck, G.M., Brook, E.J., 2007. Rapid Holocene deglaciation of the Labrador sector of the Laurentide ice sheet. J. Clim. 20, 5126–5133.
Charpentier, J., 1841. Essai sur les glaciers et sur le terrain erratique du bassin du Rhône. M. Ducloux, Lausanne (in French).
Chen, Y.X., Li, Y.K., Zhang, M., Zhang, J.C., Liu, G.N., 2011. Terrestrial cosmogenic nuclide ^{10}Be exposure ages of the samples from Wangkun till in the Kunlun Pass. J. Glaciol. Geocryol. 33, 101–109 (in Chinese with English abstract).
Clark, J., McCabe, A.M., Schnabel, C., Clark, P.U., Freeman, S., Maden, C., Xu, S., 2009a. ^{10}Be chronology of the last deglaciation of County Donegal, northwestern Ireland. Boreas 38, 111–118.
Clark, J., McCabe, A.M., Schnabel, C., Clark, P.U., McCarron, S., Freeman, S.P.H.T., Maden, C., Xu, S., 2009b. Cosmogenic ^{10}Be chronology of the last deglaciation of western Ireland, and implications for sensitivity of the Irish ice sheet to climate change. Geol. Soc. Am. Bull. 121, 3–16.
Codilean, A.T., 2006. Calculation of the cosmogenic nuclide production topographic shielding scaling factor for large areas using DEMs. Earth Surf. Process. Landf. 31, 785–794.
Corbett, L.B., Bierman, P.R., Lasher, G.E., Rood, D.H., 2015. Landscape chronology and glacial history in Thule, northwest Greenland. Quat. Sci. Rev. 109, 57–67.
Cronauer, S.L., Briner, J.P., Kelley, S.E., Zimmerman, S.R.H., Morlighem, M., 2016. ^{10}Be dating reveals early-middle Holocene age of the Drygalski moraines in central west Greenland. Quat. Sci. Rev. http://dx.doi.org/10.1016/j.quascirev.2015.08.034 (in press).
Darvill, C.M., Bentley, M.J., Stokes, C.R., 2015. Geomorphology and weathering characteristics of erratic boulder trains on Tierra del Fuego, southernmost South America: implications for dating of glacial deposits. Geomorphology 228, 382–397.
Davis, P.T., Briner, J.P., Coulthard, R.D., Finkel, R.W., Miller, G.H., 2006. Preservation of Arctic landscapes overridden by cold-based ice sheets. Quat. Res. 65, 156–163.
Di Nicola, L., Strasky, S., Schlüchter, C., Salvatore, M.C., Akçar, N., Kubik, P.W., Christl, M., Kasper, H.W., Wieler, R., Baroni, C., 2009. Multiple cosmogenic nuclides document complex Pleistocene exposure history of glacial drifts in Terra Nova Bay (northern Victoria Land, Antarctica). Quat. Res. 71, 83–92.
Dong, G.C., Yi, C.L., Caffee, M., 2014. ^{10}Be dating of boulders on moraines from the last glacial period in the Nyainqentanglha mountains. Tibet. Sci. China Earth Sci. 57, 221–231.
Dortch, J.M., Owen, L.A., Caffee, M.W., Brease, P., 2010a. Late Quaternary glaciation and equilibrium line altitude variations of the McKinley River region, central Alaska Range. Boreas 39, 233–246.
Dortch, J.M., Owen, L.A., Caffee, M.W., Li, D.W., Lowell, T.V., 2010b. Beryllium-10 surface exposure dating of glacial successions in the central Alaska Range. J. Quat. Sci. 25, 1259–1269.
Doughty, A.M., Schaefer, J.M., Putnam, A.E., Denton, G.H., Kaplan, M.R., Barrell, D.J.A., Andersen, B.G., Kelley, S.E., Finkel, R.C., Schwartz, R., 2015. Mismatch of glacier extent and summer insolation in southern Hemisphere mid-latitudes. Geology 43, 407–410.
Douglass, D.C., Singer, B.S., Kaplan, M.R., Ackert, R.P., Mickelson, D.M., Caffee, M.W., 2005. Evidence of early Holocene glacial advances in southern South America from cosmogenic surface-exposure dating. Geology 33, 237–240.
Douglass, D.C., Singer, B.S., Kaplan, M.R., Mickelson, D.M., Caffee, M.W., 2006. Cosmogenic nuclide surface exposure dating of boulders on last-glacial and late-glacial moraines, Lago Buenos Aires, Argentina: interpretive strategies and paleoclimate implications. Quat. Geochronol. 1, 43–58.
Engel, Z., Traczyk, A., Braucher, R., Woronko, B., Křížek, M., 2011. Use of ^{10}Be exposure ages and Schmidt hammer data for correlation of moraines in the Krkonoše Mountains, Poland/Czech Republic. Z. Geomorphol. 55, 175–196.
Engel, Z., Braucher, R., Traczyk, A., Laetitia, L., Arnold, M., Aumaître, G., Bourlès, D., Keddadouche, K., 2014. ^{10}Be exposure age chronology of the last glaciation in the Krkonoše Mountains, central Europe. Geomorphology 206, 107–121.
Engel, Z., Mentlík, P., Braucher, R., Minár, J., Léanni, L., Arnold, M., Aumaître, G., Bourlès, D., Keddadouche, K., 2015. Geomorphological evidence and ^{10}Be exposure ages for the last glacial maximum and deglaciation of the Velká and Malá Studená dolina valleys in the High Tatra Mountains, central Europe. Quat. Sci. Rev. 124, 106–123.
Fabel, D., Stroeven, A.P., Harbor, J., Kleman, J., Elmore, D., Fink, D., 2002. Landscape preservation under Fennoscandian ice sheets determined from in situ produced ^{10}Be and ^{26}Al. Earth Planet. Sci. Lett. 201, 397–406.
Fink, D., McKelvey, B., Hambrey, M.J., Fabel, D., Brown, R., 2006. Pleistocene deglaciation chronology of the Amery oasis and radok Lake, northern prince charles mountains, Antarctica. Earth Planet. Sci. Lett. 243, 229–243.
Fogwill, C.J., Kubik, P.W., 2005. A glacial stage spanning the Antarctic cold reversal in Torres del Paine (51°S), Chile, based on preliminary cosmogenic exposure ages. Geogr. Ann. 87A, 403–408.
Fu, P., Stroeven, A.P., Harbor, J.M., Hättestrand, C., Heyman, J., Caffee, M.W., Zhou, L.P., 2013. Paleoglaciation of shaluli shan, southeastern tibetan plateau. Quat. Sci. Rev. 64, 121–135.
García, J.L., Kaplan, M.R., Hall, B.L., Schaefer, J.M., Vega, R.M., Schwartz, R., 2012. Glacier expansion in southern Patagonia throughout the Antarctic cold reversal. Geology 40, 859–862.
Gheorghiu, D.M., Hosu, M., Corpade, C., Xu, S., 2015. Deglaciation constraints in the Parâng Mountains, southern Romania, using surface exposure dating. Quat. Int. 388, 156–167.
Gjermundsen, E.F., Briner, J.P., Akçar, N., Salvigsen, O., Kubik, P., Gantert, N., Hormes, A., 2013. Late Weichselian local ice dome configuration and chronology in northwestern Svalbard: early thinning, late retreat. Quat. Sci. Rev. 72, 112–127.
Glasser, N.F., Harrison, S., Ivy-Ochs, S., Duller, G.A.T., Kubik, P.W., 2006. Evidence from the Rio Bayo valley on the extent of the north Patagonian icefield during the late Pleistocene-Holocene transition. Quat. Res. 65, 70–77.
Glasser, N.F., Clemmens, S., Schnabel, C., Fenton, C.R., McHargue, L., 2009. Tropical glacier fluctuations in the Cordillera Blanca, Peru between 12.5 and 7.6 ka from cosmogenic ^{10}Be dating. Quat. Sci. Rev. 28, 3448–3458.
Glasser, N.F., Jansson, K.N., Goodfellow, B.W., de Angelis, H., Rodnight, H., Rood, D.H., 2011. Cosmogenic nuclide exposure ages for moraines in the Lago San Martin Valley, Argentina. Quat. Res. 75, 636–646.
Glasser, N.F., Davies, B.J., Carrivick, J.L., Rodés, A., Hambrey, M.J., Smellie, J.L., Domack, E., 2014. Ice-stream initiation, duration and thinning on James Ross Island, northern Antarctic Peninsula. Quat. Sci. Rev. 86, 78–88.
Goehring, B.M., Brook, E.J., Linge, H., Raisbeck, G.M., Yiou, F., 2008. Beryllium-10 exposure ages of erratic boulders in southern Norway and implications for the history of the Fennoscandian ice sheet. Quat. Sci. Rev. 27, 320–336.
Golledge, N.R., Fabel, D., Everest, J.D., Freeman, S., Binnie, S., 2007. First cosmogenic ^{10}Be age constraint on the timing of Younger Dryas glaciation and ice cap thickness, western Scottish highlands. J. Quat. Sci. 22, 785–791.
Gosse, J.C., Evenson, E.B., Klein, J., Lawn, B., Middleton, R., 1995. Precise cosmogenic ^{10}Be measurements in western North America: support for a global Younger Dryas cooling event. Geology 23, 877–880.
Graf, A.A., Strasky, S., Ivy-Ochs, S., Akçar, N., Kubik, P.W., Burkhard, M., Schlüchter, C., 2007. First results of cosmogenic dated pre-Last Glaciation erratics from the Montoz area, Jura Mountains, Switzerland. Quat. Int. 164–165, 43–52.
Graf, A.A., Strasky, S., Zhao, Z.Z., Akçar, N., Ivy-Ochs, S., Kubik, P.W., Christl, M., Kasper, H.U., Wieler, R., Schlüchter, C., 2008. Glacier extension on the eastern Tibetan Plateau in response to MIS 2 cooling, with a contribution to ^{10}Be and ^{21}Ne methodology (PhD thesis). In: Strasky, S. (Ed.), Glacial Response to Global Climate Changes: Cosmogenic Nuclide Chronologies from High and Low Latitudes. ETH Zürich.
Graf, A., Akçar, N., Ivy-Ochs, S., Strasky, S., Kubik, P.W., Christl, M., Burkhard, M., Wieler, R., Schlüchter, C., 2015. Multiple advances of Alpine glaciers into the Jura Mountains in the northwestern Switzerland. Swiss J. Geosci. 108, 225–238.
Håkansson, L., Briner, J., Alexanderson, H., Aldahan, A., Possnert, G., 2007a. ^{10}Be ages from central east Greenland constrain the extent of the Greenland ice sheet during the last glacial maximum. Quat. Sci. Rev. 26, 2316–2321.
Håkansson, L., Graf, A., Strasky, S., Ivy-Ochs, S., Kubik, P.W., Hjort, C., Schlüchter, C., 2007b. Cosmogenic ^{10}Be-ages from the store koldewey island, NE Greenland. Geogr. Ann. 89A, 195–202.
Håkansson, L., Alexanderson, H., Hjort, C., Möller, P., Briner, J.P., Aldahan, A., Possnert, G., 2009. Late Pleistocene glacial history of Jameson Land, central east Greenland, derived from cosmogenic ^{10}Be and ^{26}Al exposure dating. Boreas 38, 244–260.
Hallet, B., Putkonen, J., 1994. Surface dating of dynamic landforms: young boulders on aging moraines. Science 265, 937–940.
Hebenstreit, R., Ivy-Ochs, S., Kubik, P.W., Schlüchter, C., Böse, M., 2011. Lateglacial and early Holocene surface exposure ages of glacial boulders in the Taiwanese high mountain range. Quat. Sci. Rev. 30, 298–311.
Hedrick, K.A., Seong, Y.B., Owen, L.A., Caffee, M.W., Dietsch, C., 2011. Towards defining the transition in style and timing of Quaternary glaciation between the monsoon-influenced Greater Himalaya and the semi-arid Transhimalaya of Northern India. Quat. Int. 236, 21–33.
Hein, A.S., Hulton, N.R.J., Dunai, T.J., Schnabel, C., Kaplan, M.R., Naylor, M., Xu, S., 2009. Middle Pleistocene glaciation in Patagonia dated by cosmogenic-nuclide measurements on outwash gravels. Earth Planet. Sci. Lett. 286, 184–197.
Hein, A.S., Hulton, N.R.J., Dunai, T.J., Sugden, D.E., Kaplan, M.R., Xu, S., 2010. The chronology of the last glacial maximum and deglacial events in central Argentine Patagonia. Quat. Sci. Rev. 29, 1212–1227.
Hein, A.S., Dunai, T.J., Hulton, N.R.J., Xu, S., 2011. Exposure dating outwash gravels to determine the age of the greatest Patagonian glaciations. Geology 39, 103–106.
Henriksen, M., Alexanderson, H., Landvik, J.Y., Linge, H., Peterson, G., 2014. Dynamics and retreat of the late weichselian kongsfjorden ice stream, NW svalbard. Quat. Sci. Rev. 92, 235–245.
Heyman, J., Stroeven, A.P., Caffee, M.W., Hättestrand, C., Harbor, J.M., Li, Y.K., Alexanderson, H., Zhou, L.P., Hubbard, A., 2011a. Palaeoglaciology of Bayan har shan, NE tibetan plateau: exposure ages reveal a missing LGM expansion. Quat. Sci. Rev. 30, 1988–2001.
Heyman, J., Stroeven, A.P., Harbor, J., Caffee, M.W., 2011b. Too young or too old: evaluating cosmogenic exposure dating based on an analysis of compiled boulder exposure ages. Earth Planet. Sci. Lett. 302, 71–80.

Hippe, K., Ivy-Ochs, S., Kober, F., Zasadni, J., Wieler, R., Wacker, L., Kubik, P.W., Schlüchter, C., 2014. Chronology of lateglacial ice flow reorganization and deglaciation in the Gotthard Pass area, central Swiss Alps, based on cosmogenic ^{10}Be and in situ ^{14}C. Quat. Geochronol. 19, 14–26.
Hormes, A., Akçar, N., Kubik, P.W., 2011. Cosmogenic radionuclide dating indicates ice-sheet configuration during MIS 2 on Nordaustlandet, Svalbard. Boreas 40, 636–649.
Hormes, A., Gjermundsen, E.F., Rasmussen, T.L., 2013. From mountain top to the deep sea–deglaciation in 4D of the northwestern Barents Sea ice sheet. Quat. Sci. Rev. 75, 78–99.
Houmark-Nielsen, M., Linge, H., Fabel, D., Schnabel, C., Xu, S., Wilcken, K.M., Binnie, S., 2012. Cosmogenic surface exposure dating the last deglaciation in Denmark: discrepancies with independent age constraints suggest delayed periglacial landform stabilisation. Quat. Geochronol. 13, 1–17.
Hughes, P.D., Fink, D., Fletcher, W.J., Hannah, G., 2014. Catastrophic rock avalanches in a glaciated valley of the High Atlas, Morocco: ^{10}Be exposure ages reveal a 4.5 ka seismic event. Geol. Soc. Am. Bull. 126, 1093–1104.
Hughes, P.D., Glasser, N.F., Fink, D., 2016. Rapid thinning of the Welsh ice cap at 20-19 ka based on ^{10}Be ages. Quat. Res. 85, 107–117.
Ivy-Ochs, S., Schlüchter, C., Kubik, P.W., Denton, G.H., 1999. Moraine exposure dates imply synchronous younger dryas glacier advances in the Euroopean Alps and in the southern Alps of New Zealand. Geogr. Ann. 81A, 313–323.
Ivy-Ochs, S., Schäfer, J., Kubik, P.W., Synal, H.-A., Schlüchter, C., 2004. Timing of deglaciation on the northern Alpine foreland (Switzerland). Eclogae Geol. Helv. 97, 47–55.
Ivy-Ochs, S., Kerschner, H., Kubik, P.W., Schlüchter, C., 2006a. Glacier response in the European Alps to heinrich event 1 cooling: the gschnitz stadial. J. Quat. Sci. 21, 115–130.
Ivy-Ochs, S., Kerschner, H., Reuther, A., Maisch, M., Sailer, R., Schaefer, J., Kubik, P.W., Synal, H.-A., Schlüchter, C., 2006b. The timing of glacier advances in the northern European Alps based on surface exposure dating with cosmogenic ^{10}Be, ^{26}Al, ^{36}Cl, and ^{21}Ne. In: Siame, L.L., Bourlès, D.L., Brown, E.T. (Eds.), In Situ-produced Cosmogenic Nuclides and Quantification of Geological Processes. Geol. Soc. Am. Spec. Pap, vol. 415, pp. 43–60.
Ivy-Ochs, S., Kerschner, H., Reuther, A., Preusser, F., Heine, K., Maisch, M., Kubik, P.W., Schlüchter, C., 2008. Chronology of the last glacial cycle in the European Alps. J. Quat. Sci. 23, 559–573.
Johnsen, T.F., Alexanderson, H., Fabel, D., Freeman, S.P.H.T., 2009. New ^{10}Be cosmogenic ages from the Vimmerby moraine confirm the timing of Scandinavian ice sheet deglaciation in southern Sweden. Geogr. Ann. 91A, 113–120.
Jomelli, V., Khodri, M., Favier, V., Brunstein, D., Ledru, M.-P., Wagnon, P., Blard, P.-H., Sicart, J.-E., Braucher, R., Grancher, D., Bourlès, D.L., Braconnot, P., Vuille, M., 2011. Irregular tropical glacier retreat over the Holocene epoch driven by progressive warming. Nature 474, 196–199.
Jomelli, V., Favier, V., Vuille, M., Braucher, R., Martin, L., Blard, P.-H., Colose, C., Brunstein, D., He, F., Khodri, M., Bourlès, D.L., Leanni, L., Rinterknecht, V., Grancher, D., Francou, B., Ceballos, J.L., Fonseca, H., Liu, Z., Otto-Bliesner, B.L., 2014. A major advance of tropical Andean glaciers during the Antarctic cold reversal. Nature 513, 224–228.
Joy, K., Fink, D., Storey, B., Atkins, C., 2014. A 2 million year glacial chronology of the Hatherton Glacier, Antarctica and implications for the size of the East Antarctic ice sheet at the last glacial maximum. Quat. Sci. Rev. 83, 46–57.
Kaplan, M.R., Ackert, R.P., Singer, B.S., Douglass, D.C., Kurz, M.D., 2004. Cosmogenic nuclide chronology of millennial-scale glacial advances during O-isotope stage 2 in Patagonia. Geol. Soc. Am. Bull. 116, 308–321.
Kaplan, M.R., Douglass, D.C., Singer, B.S., Ackert, R.P., Caffee, M.W., 2005. Cosmogenic nuclide chronology of pre-last glacial maximum moraines at Lago Buenos Aires, 46°S, Argentina. Quat. Res. 63, 301–315.
Kaplan, M.R., Coronato, A., Hulton, N.R.J., Rabassa, J.O., Kubik, P.W., Freeman, S.P.H.T., 2007. Cosmogenic nuclide measurements in southernmost South America and implications for landscape change. Geomorphology 87, 284–301.
Kaplan, M.R., Fogwill, C.J., Sugden, D.E., Hulton, N.R.J., Kubik, P.W., Freeman, S.P.H.T., 2008. Southern Patagonian glacial chronology for the last glacial period and implications for Southern Ocean climate. Quat. Sci. Rev. 27, 284–294.
Kelley, S.E., Briner, J.P., Young, N.E., Babonis, G.S., Csatho, B., 2012. Maximum late Holocene extent of the western Greenland ice sheet during the late 20th century. Quat. Sci. Rev. 56, 89–98.
Kelly, M.A., Lowell, T.V., Applegate, P.J., Phillips, F.M., Schaefer, J.M., Smith, C.A., Kim, H., Leonard, K.C., Hudson, A.M., 2015. A locally calibrated, late glacial ^{10}Be production rate from a low-latitude, high-altitude site in the Peruvian Andes. Quat. Geochronol. 26, 70–85.
Kerschner, H., Hertl, A., Gross, G., Ivy-Ochs, S., Kubik, P.W., 2006. Surface exposure dating of moraines in the Kromer valley (Silvretta Mountains, Austria) – evidence for glacial response to the 8.2 ka event in the eastern Alps? Holocene 16, 7–15.
Kiernan, K., Fink, D., Greig, D., Mifud, C., 2010. Cosmogenic radionuclide chronology of pre-last glacial cycle moraines in the western Arthur range, southwest Tasmania. Quat. Sci. Rev. 29, 3286–3297.
Kiernan, K., McMinn, M.S., Fink, D., 2014. Topographic and microclimatic impacts on glaciation of the Denison Range, southwest Tasmania. Quat. Sci. Rev. 97, 136–147.
Laabs, B.J.C., Munroe, J.S., Rosenbaum, J.G., Refsnider, K.A., Mickelson, D.M., Singer, B.S., Caffee, M.W., 2007. Chronology of the last glacial maximum in the upper Bear River basin. Utah. Arct. Antarct. Alp. Res. 39, 537–548.
Laabs, B.J.C., Refsnider, K.A., Munroe, J.S., Mickelson, D.M., Applegate, P.J., Singer, B.S., Caffee, M.W., 2009. Latest Pleistocene glacial chronology of the Uinta Mountains: support for moisture-driven asynchrony of the last deglaciation. Quat. Sci. Rev. 28, 1171–1187.
Laabs, B.J.C., Marchetti, D.W., Munroe, J.S., Refsnider, K.A., Gosse, J.C., Lips, E.W., Becker, R.A., Mickelson, D.M., Singer, B.S., 2011. Chronology of latest Pleistocene mountain glaciation in the western Wasatch Mountains, Utah, U.S.A. Quat. Res. 76, 272–284.
Le Roy, M., 2012. Reconstitution des fluctuations glaciaires holocènes dans les Alpes occidentales: apports de la dendrochronologie et de la datation par isotopes cosmogéniques produits in situ (PhD thesis). University of Grenoble.
Lee, S.Y., Seong, Y.B., Owen, L.A., Murari, M.K., Lim, H.S., Yoon, H.I., Yoo, K.-C., 2014. Late Quaternary glaciation in the Nun-Kun massif, northwestern India. Boreas 43, 67–89.
Li, Y.K., 2013. Determining topographic shielding from digital elevation models for cosmogenic nuclide analysis: a GIS approach and field validation. J. Mt. Sci. 10, 355–362.
Li, Y.K., Liu, G.N., Chen, Y.X., Li, Y.N., Harbor, J., Stroeven, A.P., Caffee, M., Zhang, M., Li, C.C., Cui, Z.J., 2014. Timing and extent of Quaternary glaciations in the Tianger Range, eastern Tian Shan, China, investigated using ^{10}Be surface exposure dating. Quat. Sci. Rev. 98, 7–23.
Licciardi, J.M., Pierce, K.L., 2008. Cosmogenic exposure-age chronologies of Pinedale and Bull Lake glaciations in greater yellowstone and the teton range, USA. Quat. Sci. Rev. 27, 814–831.
Licciardi, J.M., Schaefer, J.M., Taggart, J.R., Lund, D.C., 2009. Holocene glacier fluctuations in the Peruvian Andes indicate northern climate linkages. Science 325, 1677–1679.
Lifton, N., Beel, C., Hättestrand, C., Kassab, C., Rogozhina, I., Heermance, R., Oskin, M., Burbank, D., Blomdin, R., Gribenski, N., Caffee, M., Goehring, B.M., Heyman, J., Ivanov, M., Li, Y.N., Li, Y.K., Petrakov, D., Usubaliev, R., Codilean, A.T., Chen, Y.X., Harbor, J., Stroeven, A.P., 2014a. Constraints on the late Quaternary glacial history of the Inylchek and Sary-Dzaz valleys from in situ cosmogenic ^{10}Be and ^{26}Al, eastern Kyrgyz Tian Shan. Quat. Sci. Rev. 101, 77–90.
Lifton, N., Sato, T., Dunai, T.J., 2014b. Scaling in situ cosmogenic nuclide production rates using analytical approximations to atmospheric cosmic-ray fluxes. Earth Planet. Sci. Lett. 386, 149–160.
Lindow, J., Castex, M., Wittman, H., Johnson, J.S., Lisker, F., Gohl, K., Spiegel, C., 2014. Glacial retreat in the Amundsen Sea sector, West Antarctica – first cosmogenic evidence from central Pine Island Bay and the Kohler Range. Quat. Sci. Rev. 98, 166–173.
Mackintosh, A., White, D., Fink, D., Gore, D.B., Pickard, J., Fanning, P.C., 2007. Exposure ages from mountain dipsticks in Mac. Robertson Land, East Antarctica, indicate little change in ice-sheet thickness since the last glacial maximum. Geology 35, 551–554.
Mangerud, J., Gosse, J., Matiouchkov, A., Dolvik, T., 2008. Glaciers in the polar Urals, Russia, were not much larger during the last global glacial maximum than today. Quat. Sci. Rev. 27, 1047–1057.
Margold, M., Stroeven, A.P., Clague, J.J., Heyman, J., 2014. Timing of terminal Pleistocene deglaciation at high elevations in southern and central British Columbia constrained by ^{10}Be exposure dating. Quat. Sci. Rev. 99, 193–202.
Margold, M., Jansen, J.D., Gurinov, A.L., Codilean, A.T., Fink, D., Preusser, F., Reznichenko, N.V., Mifsud, C., 2016. Extensive glaciation in Transbaikalia, Siberia, at the last glacial maximum. Quat. Sci. Rev. 132, 161–174.
Mathers, H., 2014. The Impact of the Minch Palaeo-ice Stream in NW Scotland: Constraining Glacial Erosion and Landscape Evolution through Geomorphology and Cosmogenic Nuclide Analysis (PhD thesis). University of Glasgow.
May, J.-H., Zech, J., Zech, R., Preusser, F., Argollo, J., Kubik, P.W., Veit, H., 2011. Reconstruction of a complex late Quaternary glacial landscape in the Cordillera de Cochabamba (Bolivia) based on a morphostratigraphic and multiple dating approach. Quat. Res. 76, 106–118.
McCarthy, A., Mackintosh, A., Rieser, U., Fink, D., 2008. Mountain glacier chronology from Boulder Lake, New Zealand, indicates MIS 4 and MIS 2 ice advances of similar extent. Arct. Antarct. Alp. Res. 40, 695–708.
McCulloch, R.D., Fogwill, C.J., Sugden, D.E., Bentley, M.J., Kubik, P.W., 2005. Chronology of the last glaciation in central strait of magellan and Bahía inútil, southernmost south America. Geogr. Ann. 87A, 289–312.
Mentlík, P., Engel, Z., Braucher, R., Léanni, L., Arnold, M., Aumaître, G., Bourlès, D., Keddadouche, K., 2013. Chronology of the late weichselian glaciation in the Bohemian Forest in central Europe. Quat. Sci. Rev. 65, 120–128.
Moran, A.P., Kerschner, H., Ivy-Ochs, S., 2016. Redating the moraines in the Kromer Valley (Silvretta Mountains) – new evidence for an early Holocene glacier advance. Holocene. http://dx.doi.org/10.1177/0959683615612571 (in press).
Moreno, P.I., Kaplan, M.R., François, J.P., Villa-Martínez, R., Moy, C.M., Stern, C.R., Kubik, P.W., 2009. Renewed glacial activity during the Antarctic cold reversal and persistence of cold conditions until 11.5 ka in southwestern Patagonia. Geology 37, 375–378.
Munroe, J.S., Laabs, B.J.C., Shakun, J.D., Singer, B.S., Mickelson, D.M., Refsnider, K.A., Caffee, M.W., 2006. Latest Pleistocene advance of alpine glaciers in the southwestern Uinta Mountains, Utah, USA: evidence for the influence of local moisture sources. Geology 34, 841–844.
Murari, M.K., Owen, L.A., Dortch, J.M., Caffee, M.W., Dietsch, C., Fuchs, M., Haneberg, W.C., Sharma, M.C., Townsend-Small, A., 2014. Timing and climatic drivers for glaciation across monsoon-influenced regions of the Himalayan-Tibetan orogen. Quat. Sci. Rev. 88, 159–182.
Murray, D.S., Carlson, A.E., Singer, B.S., Anslow, F.S., He, F., Caffee, M., Marcott, S.A., Liu, Z.Y., Otto-Bliesner, B.L., 2012. Northern Hemisphere forcing of the last

deglaciation in southern Patagonia. Geology 40, 631–634.
Nývlt, D., Braucher, R., Engel, Z., Mlčoch, B., Arnold, M., Aumaître, G., Bourlès, D., Keddadouche, K., 2014. Timing of the northern Prince Gustav ice stream retreat and the deglaciation of northern James Ross Island, Antarctic Peninsula during the last glacial–interglacial transition. Quat. Res. 82, 441–449.
Owen, L.A., Spencer, J.Q., Ma, H.Z., Barnard, P.L., Derbyshire, E., Finkel, R.C., Caffee, M.W., Nian, Z.Y., 2003. Timing of late quaternary glaciation along the southwestern slopes of the Qilian Shan, Tibet. Boreas 32, 281–291.
Owen, L.A., Finkel, R.C., Barnard, P.L., Ma, H.Z., Asahi, K., Caffee, M.W., Derbyshire, E., 2005. Climatic and topographic controls on the style and timing of late Quaternary glaciation throughout Tibet and the Himalaya defined by ^{10}Be cosmogenic radionuclide surface exposure dating. Quat. Sci. Rev. 24, 1391–1411.
Owen, L.A., Caffee, M.W., Bovard, K.R., Finkel, R.C., Sharma, M.C., 2006. Terrestrial cosmogenic nuclide surface exposure dating of the oldest glacial successions in the Himalayan orogen: ladakh Range, northern India. Geol. Soc. Am. Bull. 118, 383–392.
Owen, L.A., Robinson, R., Benn, D.I., Finkel, R.C., Davis, N.K., Yi, C.L., Putkonen, J., Li, D.W., Murray, A.S., 2009. Quaternary glaciation of Mount Everest. Quat. Sci. Rev. 28, 1412–1433.
Owen, L.A., Yi, C.L., Finkel, R.C., Davis, N.K., 2010. Quaternary glaciation of gurla mandhata (Naimon'anyi). Quat. Sci. Rev. 29, 1817–1830.
Owen, L.A., Chen, J., Hedrick, K.A., Caffee, M.W., Robinson, A.C., Schoenbohm, L.M., Yuan, Z.D., Li, W.Q., Imrecke, D.B., Liu, J.F., 2012. Quaternary glaciation of the Tashkurgan Valley, southeast Pamir. Quat. Sci. Rev. 47, 56–72.
Pendleton, S.L., Ceperley, E.G., Briner, J.P., Kaufman, D.S., Zimmerman, S., 2015. Rapid and early deglaciation in the central Brooks Range, arctic Alaska. Geology 43, 419–422.
Phillips, W.M., Hall, A.M., Ballantyne, C.K., Binnie, S., Kubik, P.W., Freeman, S., 2008. Extent of the last ice sheet in northern Scotland tested with cosmogenic ^{10}Be exposure ages. J. Quat. Sci. 23, 101–107.
Phillips, F.M., Argento, D.C., Balco, G., Caffee, M.W., Clem, J., Dunai, T.J., Finkel, R., Goehring, B., Gosse, J.C., Hudson, A.M., Jull, A.J.T., Kelly, M.A., Kurz, M., Lal, D., Lifton, N., Marrero, S.M., Nishiizumi, K., Reedy, R.C., Schaefer, J., Stone, J.O.H., Swanson, T., Zreda, M.G., 2016a. The CRONUS-Earth project: a synthesis. Quat. Geochronol. 31, 119–154.
Phillips, F.M., Kelly, M.A., Hudson, A.M., Stone, J.O.H., Schaefer, J., Marrero, S.M., Fifield, L.K., Finkel, R., Lowell, T., 2016b. CRONUS-Earth calibration samples from the Huancané II moraines, Quelccaya ice cap, Peru. Quat. Geochronol. 31, 220–236.
Pratt-Sitaula, B., Burbank, D.W., Heimsath, A.M., Humphrey, N.F., Oskin, M., Putkonen, J., 2011. Topographic control of asynchronous glacial advances: a case study from Annapurna. Nepal. Geophys. Res. Lett. 38, L24502.
Putkonen, J., Swanson, T., 2003. Accuracy of cosmogenic ages for moraines. Quat. Res. 59, 255–261.
Putnam, A.E., Denton, G.H., Schaefer, J.M., Barrell, D.J.A., Andersen, B.G., Finkel, R.C., Schwartz, R., Doughty, A.M., Kaplan, M.R., Schlüchter, C., 2010a. Glacier advance in southern middle-latitudes during the Antarctic cold reversal. Nat. Geosci. 3, 700–704.
Putnam, A.E., Schaefer, J.M., Barrell, D.J.A., Vandergoes, M., Denton, G.H., Kaplan, M.R., Finkel, R.C., Schwartz, R., Goehring, B.M., Kelley, S.E., 2010b. In situ cosmogenic ^{10}Be production-rate calibration from the Southern Alps, New Zealand. Quat. Geochronol. 5, 392–409.
Putnam, A.E., Schaefer, J.M., Denton, G.H., Barrell, D.J.A., Finkel, R.C., Andersen, B.G., Schwartz, R., Chinn, T.J.H., Doughty, A.M., 2012. Regional climate control of glaciers in New Zealand and Europe during the pre-industrial Holocene. Nat. Geosci. 5, 627–630.
Putnam, A.E., Schaefer, J.M., Denton, G.H., Barrell, D.J.A., Andersen, B.G., Koffman, T.N.B., Rowan, A.V., Finkel, R.C., Rood, D.H., Schwartz, R., Vandergoes, M.J., Plummer, M.A., Brocklehurst, S.H., Kelley, S.E., Ladig, K.L., 2013a. Warming and glacier recession in the rakaia valley, southern Alps of New Zealand, during heinrich stadial 1. Earth Planet. Sci. Lett. 382, 98–110.
Putnam, A.E., Schaefer, J.M., Denton, G.H., Barrell, D.J.A., Birkel, S.D., Andersen, B.G., Kaplan, M.R., Finkel, R.C., Schwartz, R., Doughty, A.M., 2013b. The last glacial maximum at 44°S documented by a ^{10}Be moraine chronology at Lake Ohau, southern Alps of New Zealand. Quat. Sci. Rev. 62, 114–141.
Rades, E.F., Hetzel, R., Strobl, M., Xu, Q., Ding, L., 2015. Defining rates of landscape evolution in a south Tibetan graben with in situ-produced cosmogenic ^{10}Be. Earth Surf. Process. Landf. 40, 1862–1876.
Reber, R., Akçar, N., Ivy-Ochs, S., Tikhomirov, D., Burkhalter, R., Zahno, C., Lüthold, A., Kubik, P.W., Vockenhuber, C., Schlüchter, C., 2014a. Timing of retreat of the Reuss Glacier (Switzerland) at the end of the last glacial maximum. Swiss J. Geosci. 107, 293–307.
Reber, R., Akçar, N., Yesilyurt, S., Yavuz, V., Tikhomirov, D., Kubik, P.W., Schlüchter, C., 2014b. Glacier advances in northeastern Turkey before and during the global last glacial maximum. Quat. Sci. Rev. 101, 177–192.
Refsnider, K.A., Laabs, B.J.C., Plummer, M.A., Mickelson, D.M., Singer, B.S., Caffee, M.W., 2008. Last glacial maximum climate inferences from cosmogenic dating and glacier modeling of the western Uinta ice field, Uinta Mountains. Utah. Quat. Res. 69, 130–144.
Reuther, A.U., 2007. Surface Exposure Dating of Glacial Deposits from the Last Glacial Cycle – Evidence from the Eastern Alps, the Bavarian Forest, the Southern Carpathians and the Altai Mountains, vol. 21. Relief Boden Paläoklima, pp. 1–213.
Reuther, A.U., Urdea, P., Geiger, C., Ivy-Ochs, S., Niller, H.-P., Kubik, P.W., Heine, K., 2007. Late Pleistocene glacial chronology of the Pietrele Valley, Retezat Mountains, southern Carpathians constrained by ^{10}Be exposure ages and pedological investigations. Quat. Int. 164–165, 151–169.
Reuther, A.U., Fiebig, M., Ivy-Ochs, S., Kubik, P.W., Reitner, J.M., Jerz, H., Heine, K., 2011. Deglaciation of a large piedmont lobe glacier in comparison with a small mountain glacier – new insight from surface exposure dating. Two studies from SE Germany. Eiszeitalt. Ggw. Quat. Sci. J. 60, 248–269.
Rinterknecht, V.R., Clark, P.U., Raisbeck, G.M., Yiou, F., Brook, E.J., Tschudi, S., Lunkka, J.P., 2004. Cosmogenic ^{10}Be dating of the Salpausselkä I moraine in southwestern Finland. Quat. Sci. Rev. 23, 2283–2289.
Rinterknecht, V.R., Marks, L., Piotrowski, J.A., Raisbeck, G.M., Yiou, F., Brook, E.J., Clark, P.U., 2005. Cosmogenic ^{10}Be ages on the Pomeranian moraine. Pol. Boreas 34, 186–191.
Rinterknecht, V., Gorokhovich, Y., Schaefer, J., Caffee, M., 2009. Preliminary ^{10}Be chronology for the last deglaciation of the western margin of the Greenland ice sheet. J. Quat. Sci. 24, 270–278.
Rother, H., 2006. Late Pleistocene Glacial Geology of the Hope-Waiau Valley System in North Canterbury, New Zealand (PhD thesis). University of Canterbury.
Rother, H., Fink, D., Shulmeister, J., Mifsud, C., Evans, M., Pugh, J., 2014a. The early rise and late demise of New Zealand's last glacial maximum. Proc. Natl. Acad. Sci. 111, 11630–11635.
Rother, H., Lehmkuhl, F., Fink, D., Nottebaum, V., 2014b. Surface exposure dating reveals MIS-3 glacial maximum in the Khangai Mountains of Mongolia. Quat. Res. 82, 297–308.
Rother, H., Shulmeister, J., Fink, D., Alexander, D., Bell, D., 2015. Surface exposure chronology of the Waimakariri glacial sequence in the Southern Alps of New Zealand: implications for MIS-2 ice extent and LGM glacial mass balance. Earth Planet. Sci. Lett. 429, 69–81.
Ruszkiczay-Rüdiger, Z., Kern, Z., Urdea, P., Braucher, R., Madarász, B., Schimmelpfennig, I., Arnold, M., Aumaître, G., Bourlès, D., Keddadouche, K., 2016. Revised deglaciation history of the Pietrele-Stânişoara glacial complex, Retezat Mts, southern Carpathians, Romania. Quat. Int. http://dx.doi.org/10.1016/j.quaint.2015.10.085 (in press).
Sagredo, E.A., Moreno, P.I., Villa-Martínez, R., Kaplan, M.R., Kubik, P.W., Stern, C.R., 2011. Fluctuations of the Última Esperanza ice lobe (52°S), Chilean Patagonia, during the last glacial maximum and termination 1. Geomorphology 125, 92–108.
Saha, S., Sharma, M.C., Murari, M.K., Owen, L.A., Caffee, M.W., 2016. Geomorphology, sedimentology and minimum exposure ages of streamlined subglacial landforms in the NW Himalaya, India. Boreas. http://dx.doi.org/10.1111/bor.12153 (in press).
Schaefer, J.M., Denton, G.H., Barrell, D.A., Ivy-Ochs, S., Kubik, P.W., Andersen, B.G., Phillips, F.M., Lowell, T.V., Schlüchter, C., 2006. Near-synchronous interhemispheric termination of the last glacial maximum in mid-latitudes. Science 312, 1510–1513.
Scherler, D., Bookhagen, B., Strecker, M.R., von Blanckenburg, F., Rood, D., 2010. Timing and extent of late Quaternary glaciation in the western Himalaya constrained by ^{10}Be moraine dating in Garhwal, India. Quat. Sci. Rev. 29, 815–831.
Schildgen, T.F., 2000. Fire and Ice: the Geomorphic History of Middle Boulder Creek as Determined by Isotopic Dating Techniques, Colorado Front Range (Bs thesis). Williams College.
Schindelwig, I., Akçar, N., Kubik, P.W., Schlüchter, C., 2012. Lateglacial and early Holocene dynamics of adjacent valley glaciers in the western Swiss Alps. J. Quat. Sci. 27, 114–124.
Seong, Y.B., Owen, L.A., Bishop, M.P., Bush, A., Clendon, P., Copland, L., Finkel, R., Kamp, U., Shroder, J.F., 2007. Quaternary glacial history of the central Karakoram. Quat. Sci. Rev. 26, 3384–3405.
Seong, Y.B., Owen, L.A., Yi, C.L., Finkel, R.C., 2009. Quaternary glaciation of Muztag Ata and Kongur Shan: evidence for glacier response to rapid climate changes throughout the late glacial and Holocene in westernmost Tibet. Geol. Soc. Am. Bull. 121, 348–365.
Shakun, J.D., Clark, P.U., He, F., Lifton, N.A., Liu, Z.Y., Otto-Bliesner, B.L., 2015. Regional and global forcing of glacier retreat during the last deglaciation. Nat. Commun. 6, 8059.
Shulmeister, J., Fink, D., Augustinus, P.C., 2005. A cosmogenic nuclide chronology of the last glacial transition in north-west Nelson, New Zealand – new insights in southern hemisphere climate forcing during the last deglaciation. Earth Planet. Sci. Lett. 233, 455–466.
Shulmeister, J., Fink, D., Hyatt, O.M., Thackray, G.D., Rother, H., 2010. Cosmogenic ^{10}Be and ^{26}Al exposure ages of moraines in the Rakaia Valley, New Zealand and the nature of the last termination in New Zealand glacial systems. Earth Planet. Sci. Lett. 297, 558–566.
Smith, J.A., Rodbell, D.T., 2010. Cross-cutting moraines reveal evidence for North Atlantic influence on glaciers in the tropical Andes. J. Quat. Sci. 25, 243–248.
Smith, J.A., Finkel, R.C., Farber, D.L., Rodbell, D.T., Seltzer, G.O., 2005a. Moraine preservation and boulder erosion in the tropical Andes: interpreting old surface exposure ages in glaciated valleys. J. Quat. Sci. 20, 735–758.
Smith, J.A., Seltzer, G.O., Farber, D.L., Rodbell, D.T., Finkel, R.C., 2005b. Early local last glacial maximum in the tropical Andes. Science 308, 678–681.
Standell, M.R., 2014. Lateglacial (Younger Dryas) Glaciers and Ice-sheet Deglaciation in the Cairngorm Mountains, Scotland: Glacier Reconstructions and Their Palaeoclimatic Implications (PhD thesis). Loughborough University.
Storey, B.C., Fink, D., Hood, D., Joy, K., Shulmeister, J., Riger-Kusk, M., Stevens, M.I., 2010. Cosmogenic nuclide exposure age constraints on the glacial history of the Lake Wellman area, Darwin Mountains, Antarctica. Antarct. Sci. 22, 603–618.
Strasky, S., Oberholzer, P., Meyer, K.-D., Baur, H., Ivy-Ochs, S., Kubik, P.W., Wieler, R.,

Schlüchter, C., 2006. Surface exposure dating of two erratic boulders from Niedersachsen - evidence of an old Fennoscandian ice sheet advance in northern Germany. Arch. Geschiebekd 5, 283–292 (in German, English abstract).
Strasky, S., Graf, A.A., Zhao, Z.Z., Kubik, P.W., Baur, H., Schlüchter, C., Wieler, R., 2009. Late glacial ice advances in southeast Tibet. J. Asian Earth Sci. 34, 458–465.
Stroeven, A.P., Fabel, D., Codilean, A.T., Kleman, J., Clague, J.J., Miguens-Rodriguez, M., Xu, S., 2010. Investigating the glacial history of the northern sector of the Cordilleran ice sheet with cosmogenic ^{10}Be concentrations in quartz. Quat. Sci. Rev. 29, 3630–3643.
Stroeven, A.P., Fabel, D., Margold, M., Clague, J.J., Xu, S., 2014. Investigating absolute chronologies of glacial advances in the NW sector of the Cordilleran ice sheet with terrestrial in situ cosmogenic nuclides. Quat. Sci. Rev. 92, 429–443.
Svendsen, J.I., Briner, J.P., Mangerud, J., Young, N.E., 2015. Early break-up of the Norwegian channel ice stream during the last glacial maximum. Quat. Sci. Rev. 107, 231–242.
Tschudi, S., Ivy-Ochs, S., Schlüchter, C., Kubik, P., Rainio, H., 2000. ^{10}Be dating of younger dryas salpausselkä I formation in Finland. Boreas 29, 287–293.
Tschudi, S., Schäfer, J.M., Zhao, Z.Z., Wu, X.H., Ivy-Ochs, S., Kubik, P.W., Schlüchter, C., 2003. Glacial advances in tibet during the younger dryas? evidence from cosmogenic ^{10}Be, ^{26}Al, and ^{21}Ne. J. Asian Earth Sci. 22, 301–306.
Ullman, D.J., Carlson, A.E., Clark, P.U., Cuzzone, J., Winsor, K., Caffee, M., 2013. Abrupt collapse of the labrador dome of the laurentide ice sheet linked to 8.2 ka event (PhD thesis). In: Ullman, D.J. (Ed.), Dismantling the Laurentide Ice Sheet: Refining the Chronology and Mechanisms of Deglaciation. University of Wisconsin-Madison.
Wang, J., Kassab, C., Harbor, J.M., Caffee, M.W., Cui, H., Zhang, G.L., 2013. Cosmogenic nuclide constraints on late Quaternary glacial chronology on the Dalijia Shan, northeastern Tibetan Plateau. Quat. Res. 79, 439–451.
Ward, B.C., Bond, J.D., Gosse, J.C., 2007. Evidence for a 55–50 ka (early Wisconsin) glaciation of the Cordilleran ice sheet, Yukon territory, Canada. Quat. Res. 68, 141–150.
Wesnousky, S.G., Aranguren, R., Rengifo, M., Owen, L.A., Caffee, M.W., Murari, M.K., Pérez, O.J., 2012. Toward quantifying geomorphic rates of crustal displacement, landscape development, and the age of glaciation in the Venezuelan Andes. Geomorphology 141–142, 99–113.
White, D.A., Fink, D., 2014. Late Quaternary glacial history constrains glacio-isostatic rebound in Enderby Land, East Antarctica. J. Geophys. Res. Earth Surf. 119, 401–413.
White, D.A., Fink, D., Gore, D.B., 2011. Cosmogenic nuclide evidence for enhanced sensitivity of an East Antarctic ice stream to change during the last deglaciation. Geology 39, 23–26.
Wirsig, C., Zasadni, J., Ivy-Ochs, S., Christl, M., Kober, F., Schlüchter, C., 2016. A deglaciation model of the Oberhasli, Switzerland. J. Quat. Sci. 31, 46–59.
Yamane, M., Yokoyama, Y., Miura, H., Maemoku, H., Iwasaki, S., Matsuzaki, H., 2011. The last deglacial history of Lützow-Holm Bay, East Antarctica. J. Quat. Sci. 26, 3–6.
Young, N.E., Briner, J.P., Kaufman, D.S., 2009. Late pleistocene and holocene glaciation of the fish Lake valley, northeastern Alaska range, Alaska. J. Quat. Sci. 24, 677–689.
Young, N.E., Briner, J.P., Axford, Y., Csatho, B., Babonis, G.S., Rood, D.H., Finkel, R.C., 2011a. Response of a marine-terminating Greenland outlet glacier to abrupt cooling 8200 and 9300 years ago. Geophys. Res. Lett. 38, L4701.
Young, N.E., Briner, J.P., Stewart, H.A.M., Axford, Y., Csatho, B., Rood, D.H., Finkel, R.C., 2011b. Response of jakobshavn isbræ, Greenland, to holocene climate change. Geology 39, 131–134.
Young, N.E., Briner, J.P., Rood, D.H., Finkel, R.C., 2012. Glacier extent during the younger dryas and 8.2-ka event on Baffin Island, arctic Canada. Science 337, 1330–1333.
Young, N.E., Briner, J.P., Rood, D.H., Finkel, R.C., Corbett, L.B., Bierman, P.R., 2013a. Age of the Fjord Stade moraines in the Disko Bugt region, western Greenland, and the 9.3 and 8.2 ka cooling events. Quat. Sci. Rev. 60, 76–90.
Young, N.E., Schaefer, J.M., Briner, J.P., Goehring, B.M., 2013b. A ^{10}Be production-rate calibration for the Arctic. J. Quat. Sci. 28, 515–526.
Zahno, C., Akçar, N., Yavuz, V., Kubik, P.W., Schlüchter, C., 2009. Surface exposure dating of late pleistocene glaciations at the dedegöl mountains (Lake Beyşehir, SW Turkey). J. Quat. Sci. 24, 1016–1028.
Zahno, C., Akçar, N., Yavuz, V., Kubik, P.W., Schlüchter, C., 2010. Chronology of late pleistocene glacier variations at the uludağ mountain, NW Turkey. Quat. Sci. Rev. 29, 1173–1187.
Zech, R., Kull, C., Kubik, P.W., Veit, H., 2007. LGM and late glacial glacier advances in the Cordillera Real and Cochabamba (Bolivia) deduced from ^{10}Be surface exposure dating. Clim. Past. 3, 623–635.
Zech, J., Zech, R., Kubik, P.W., Veit, H., 2009. Glacier and climate reconstruction at Tres Lagunas, NW Argentina, based on ^{10}Be surface exposure dating and lake sediment analyses. Palaeogeogr. Palaeoclimatol. Palaeoecol. 284, 180–190.
Zech, J., Zech, R., May, J.-H., Kubik, P.W., Veit, H., 2010. Lateglacial and early Holocene glaciation in the tropical Andes caused by La Niña-like conditions. Palaeogeogr. Palaeoclimatol. Palaeoecol. 293, 248–254.